International Journal of Mechanical, Industrial and Aerospace Sciences
ISSN: 2517-9950
Vol:9, No:10, 2015

Molecular Dynamics Simulation for Buckling Analysis at Nanocomposite Beams

Babak Safaei, A. M. Fattahi

***Abstract*—**In the present study we have investigated axial buckling characteristics of nanocomposite beams reinforced by single-walled carbon nanotubes (SWCNTs). Various types of beam theories including Euler-Bernoulli beam theory, Timoshenko beam theory and Reddy beam theory were used to analyze the buckling behavior of carbon nanotube-reinforced composite beams. Generalized differential quadrature (GDQ) method was utilized to discretize the governing differential equations along with four commonly used boundary conditions. The material properties of the nanocomposite beams were obtained using molecular dynamic (MD) simulation corresponding to both short-(10,10) SWCNT and long-(10,10) SWCNT composites which were embedded by amorphous polyethylene matrix. Then the results obtained directly from MD simulations were matched with those calculated by the mixture rule to extract appropriate values of carbon nanotube efficiency parameters accounting for the scale-dependent material properties. The selected numerical results were presented to indicate the influences of nanotube volume fractions and end supports on the critical axial buckling loads of nanocomposite beams relevant to long- and short-nanotube composites.

***Keywords*—**Nanocomposites, molecular dynamics simulation, axial buckling, generalized differential quadrature (GDQ).

I. Introduction

THE promise of a new generation in diverse engineering, materials science, and reinforced composite structures was inspired by the discovery of carbon nanotubes by Iijima in 1991 [1] due to the superior mechanical and physical properties of carbon nanotubes over other known materials. One of the most useful applications of this new material is its use as strong, light-weight and high-toughness fibers for nanocomposite structures. A large number of theoretical and experimental researches using carbon nanotubes as reinforcing fibers have been conducted.

Liao and Li [2] conducted molecular mechanics simulations to study the interfacial characteristics of polystyrene-nanotube interface. They noted that on relaxing the structure without applying any external force or displacement, there was a slight decrease in the nanotube diameter. Wei et al. [3] investigated the effect of chemical bondings between the carbon nanotube and polymer on effective load transfer in the composites. They observed better load transfer in case of double site bonding and higher shear strain. Lau studied by the load transfer properties between carbon nanotubes and polymer using theoretical models [4]. They found that the maximum shear stress for pullout of a single-walled carbon nanotube (SWCNT) was comparatively higher than that of a multi-walled carbon nanotube. Hammel et al. [5] concentrated on the production and improvement of vapor grown carbon fibers for composite applications. Han and Elliot [6] conducted classical molecular dynamics (MD) simulations of model polymer/carbon nanotube composites constructed by embedding an armchair SWCNT into methyl methacrylate polymer matrix. By comparing the simulation results with the macroscopic mixture rule for composite systems, they showed that for strong interfacial interactions, there could be large deviations of the results from the mixture rule rule.

In this work, buckling behavior of nanocomposite beams which were reinforced by (10,10) armchair SWCNTs embedded in amorphous polyethylene was investigated based on the various elastic beam theories [7]. Generalized differential quadrature (GDQ) method was utilized to discretize the governing differential equations along with four sets of end supported including simply supported-simply supported, clamped-clamped, clamped-simply supported, and clamped-free. Then the material properties calculated by the beam theories in conjunction with the mixture rule were fitted with those obtained directly from MD simulations to extract consistent values of carbon nanotube efficiency parameters accounting for the scale-dependent material properties corresponding to both short and long carbon nanotube reinforcements.

II. Overview of Different Beam Theories

There are various beam theories to describe the behavior of beams. Consider a straight uniform beam with the length L and rectangular cross-section of thickness h. A coordinate system (x, y, z) was introduced on the central axis of the beam, whereas the x axis was taken along the length of the beam, the y axis was in the width direction and the z axis was taken along the depth (height) direction. Also, the origin of the coordinate system was selected at the left end of the beam. It was assumed that the deformations of the beam took place in the x-z plane, so the displacement components (u_1, u_2, u_3) along the axis (x, y, z) depended only on the x and z coordinates and time t. In a general form, the following displacement field could be written as:

$$u_1(x,z,t) = -z\frac{\partial w(x,t)}{\partial x} + \psi(z)\left(\frac{\partial w(x,t)}{\partial x} + \varphi(x,t)\right)$$

Babak Safaei is with the Department of Engineering, East Azarbayjan Science and Research Branch, Islamic Azad University, Tabriz, Iran and Department of Mechanical Engineering, Tabriz Branch, Islamic Azad University, Tabriz, Iran (e-mail: Babak.safaei.me@gmail.com).

Ashghar Mohammadpour Fattahi is with the Department of Mechanical Engineering, Tabriz Branch, Islamic Azad University, Tabriz, Iran (corresponding author to provide phone: +98914 114 7711; fax: +98413 325 0940 e-mail: a.fattahi@iaut.ac.ir).

$$u_2(x,z,t) = 0 \quad (1)$$

$$u_3(x,z,t) = w(x,t)$$

where w and φ were the transverse displacement and angular displacement of the beam, respectively, and $\psi(z)$ was the shape function as follows:

For Euler-Bernoulli beam theory (EBT): $\psi(z) = 0$

For Timoshenko beam theory (TBT): $\psi(z) = z$

For Reddy beam theory (RBT): $\psi(z) = z - \frac{4z^3}{3h^2}$

In this study, it was assumed that the carbon nanotube-reinforced composite was made of a mixture of (10,10) armchair SWCNT and polyethylene matrix with isotropic behavior. It was shown that carbon nanotube-reinforced composites had anisotropic material properties. On the basis of the mixture rule, the effective values of Young's modulus and shear modulus of carbon-nanotube-reinforced composite could be evaluated as [8]

$$E_{11} = \vartheta_1 V_{CNT} E_{11}^{CNT} + V_m E^m \quad (2a)$$

$$\frac{\vartheta_2}{E_{22}} = \frac{V_{CNT}}{E_{22}^{CNT}} + \frac{V_m}{E^m} \quad (2b)$$

$$\frac{\vartheta_3}{G_{12}} = \frac{V_{CNT}}{G_{12}^{CNT}} + \frac{V_m}{G^m} \quad (2c)$$

where $E_{11}^{CNT}, E_{22}^{CNT}, and\ G_{12}^{CNT}$ were longitudinal Young's modulus, transverse Young's modulus, and shear modulus of the carbon nanotube, respectively; $E^m, and\ G^m$ were Young's modulus and shear modulus of the isotropic matrix, respectively; and $V_{CNT}, and\ V_m$ were the volume fractions of carbon nanotube and matrix, respectively and were correlated by:

$$V_{CNT} + V_m = 1 \quad (3)$$

The coefficients $\vartheta_1, \vartheta_2, \vartheta_3$ were the carbon nanotube efficiency parameters to incorporate the scale-dependent characteristic of material properties which were determined with the results obtained directly from MD simulations.

III. Generalized Differential Quadrature Method

The GDQ method is one of the most efficient numerical techniques to solve various boundary value problems. Recently, many researchers have suggested the application of the generalized differential quadrature (GDQ) method to analyze nanostructures [9]-[14]. This method has shown superb accuracy, efficiency, convenience and great potential in solving complicated partial differential equations. The basic idea of the differential quadrature method lies in the approximation of the partial derivative of a function with respect to a coordinate at a discrete point as a weighted linear sum of the function values at all discrete points along that coordinate direction. Let $\frac{\partial^r f}{\partial x^r}$ be the r th derivative of a function $f(x)$ which can be represented as a linear sum of the function values:

$$\left.\frac{\partial^r f(x)}{\partial x^r}\right|_{x=x_P} = \sum_{Q=1}^{n} A_{PQ}^{(r)} f(x_P) \quad (4)$$

where n is the number of total discrete grid points used in the approximation process and $A_{PQ}^{(r)}$ is weighting coefficients.

The weighting coefficients of the first derivative were determined by:

$$A_{PQ}^{(1)} = \frac{M(x_P)}{(x_P - x_Q)M(x_Q)} (P, Q = 1,2,\ldots,n;\ P \neq Q) \quad (5)$$

where

$$M(x_P) = \prod_{Q=1;Q\neq P}^{n} (x_P - x_Q) \quad (6)$$

The weighting coefficients of higher-order derivatives could be obtained through the following recurrence relation:

$$A_{PQ}^{(r)} = \begin{cases} r\left[A_{PQ}^{(r-1)} A_{PQ}^{(1)} - \frac{A_{PQ}^{(r-1)}}{x_p - x_q}\right], & P \neq Q \\ -\sum_{Q=1}^{n} A_{PQ}^{(r)}, & P = Q \end{cases} \quad (7)$$

By applying the GDQ method, the discrete counterparts of constitutive differential equations corresponding to each type of beam theory at the r th given point could be expressed as

For Euler-Bernoulli beam theory:

$$\frac{E_{11}I}{(1-\nu^2)} \sum_{s=1}^{n} A_{rs}^{(4)} W_s - P \sum_{s=1}^{n} A_{rs}^{(2)} W_s = 0 \quad (8)$$

For Timoshenko beam theory:

$$(\kappa G_{12} A - P) \sum_{s=1}^{n} A_{rs}^{(2)} W_s + \kappa G_{12} A \sum_{s=1}^{n} A_{rs}^{(1)} \phi_s = 0 \quad (9a)$$

$$-\kappa G_{12} A \sum_{s=1}^{n} A_{rs}^{(1)} W_s + \frac{E_{11}I}{(1-\nu^2)} \sum_{s=1}^{n} A_{rs}^{(2)} \phi_s - \kappa G_{12} A \phi_r = 0 \quad (9b)$$

For Reddy beam theory:

$$\left(\frac{8G_{12}A}{15} - P\right) \sum_{s=1}^{n} A_{rs}^{(2)} W_s + \frac{16E_{11}I}{105(1-\nu^2)} \sum_{s=1}^{n} A_{rs}^{(3)} \phi_s + \frac{8G_{12}A}{15} \sum_{s=1}^{n} A_{rs}^{(1)} \phi_s = 0 \quad (10a)$$

$$-\frac{16E_{11}I}{105(1-\nu^2)} \sum_{s=1}^{n} A_{rs}^{(3)} W_s - \frac{8G_{12}A}{15} \sum_{s=1}^{n} A_{rs}^{(1)} W_s + \frac{16E_{11}I}{105(1-\nu^2)} \sum_{s=1}^{n} A_{rs}^{(2)} \phi_s - \frac{8G_{12}A}{15} \phi_r = 0 \quad (10b)$$

IV. Molecular Dynamics Simulation

The application of MD simulation is considered to be one of the most accurate methods to describe an atomic system which has the capability of handling simulations involving large numbers of atoms, allowing more complicated dynamic systems to be modeled in an approximately short period of time when compared with *ab* initio methods. Hanasaki et al. [15] conducted MD simulation of the molecular flow inside a modeled carbon nanotube junction as a strong gravitational field and periodic boundary conditions were applied in the flow direction. Han and Elliott presented MD simulations of

model polymer/carbon nanotube composites with different volume fraction [6]. The simulation results supported the idea that it is possible to use carbon nanotubes to mechanically reinforce an appropriate polymer matrix, especially in the longitudinal direction of the nanotube. Bi et al. [16] studied the thermal conductivity of SWCNTs depending on tube length and temperature based on MD simulation. They demonstrated that the vacancy scattering on phonons was stronger than the isotropic atom which caused more reduction of lattice thermal conductivity of carbon nanotubes.

In this work, unidirectional carbon nanotube-polymer nanocomposites were simulated using the molecular dynamics simulator "NanoHive" [17]. NanoHive is a free open source MD simulator with certain features that can be used to model different loading conditions of nanostructures [17]. Two types of composites were considered including long-(10,10) SWCNT composite and short-(10,10) SWCNT composite both of which were surrounded by amorphous polyethylene matrix (Fig. 1). As shown in Fig. 2, a simulation cell with approximate dimensions of $5 \times 5 \times 10\ nm$ was utilized for all simulations which were established using the Adaptive Intermolecular Reactive Empirical Bond Order (AIREBO) potential [18]. The AIREBO potential is an extension of the commonly used REBO potential which is developed for solid carbon and hydrocarbon molecules [18]. It includes covalent bonding interactions represented by REBO potential as well as the Lennard-Jones terms and torsional interactions as

$$U^{AIREBO} = \frac{1}{2}\sum_{i}\sum_{j\neq i}\left(U_{ij}^{REBO} + U_{ij}^{LJ} + \sum_{k\neq i,j}\sum_{p\neq i,j,k} U_{kijp}^{Torsional}\right) \quad (11)$$

All MD simulations presented here were performed at room temperature (300 Kelvin). The van Gunstern-Berendsen thermostat [18] was implemented such that the scaling factor was used after each step of the MD simulation; the velocities of the atoms of the system were scaled while the average kinetic energy remained approximately constant. A time step of $0.5\ fs$ was selected with about 2000 numbers of steps to simulate deformations of the MD cell under longitudinal and transverse strain.

Longitudinal and transverse strains were applied to the MD cell, by mathematically changing the coordinates of the atoms to an extended strained condition according to Fig. 3. Then, employing NanoHive simulator, various time steps to relax the system of atoms to their equilibrium position were set up to enable the MD cell to reache the equilibrium configuration. This procedure was repeated for different values of the tensile strain as well as for 5% value of the strain. The stress-strain curves of the MD cells were obtained which showed the values of Young's modulus in the longitudinal and transverse directions. The values of Young's modulus obtained directly from the MD simulations are given in Table I corresponding to both longitudinal and transverse directions and different values of carbon nanotube volume fraction.

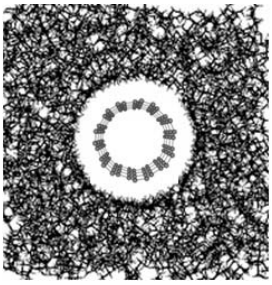

Fig. 1 (10,10) SWCNT embedded in an amorphous polyethylene

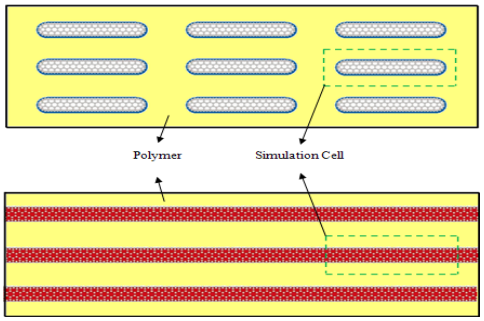

Fig. 2 Schematic MD simulation cell for both of short-SWCNT and long-SWCNT composites

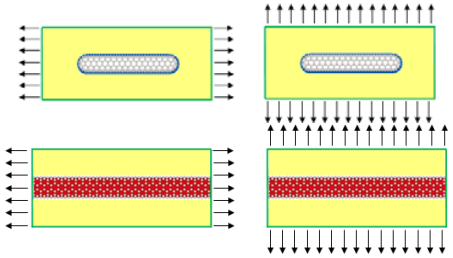

Fig. 3 Applied longitudinal and transverse strains to the MD simulation cell

TABLE I
MD RESULTS FOR THE ELASTIC MODULI OF SWCNT-REINFORCED COMPOSITES

Carbon nanotube volume fraction	Short-carbon nanotube composite		Long-carbon nanotube composite	
	Longitudinal modulus (GPa)	Transverse modulus (GPa)	Longitudinal modulus (GPa)	Transverse modulus (GPa)
0%	3.22	3.22	3.22	3.22
5%	3.82	3.45	67.79	3.93
10%	5.56	4.44	101.02	5.10
15%	8.39	6.38	154.55	7.38
20%	13.51	7.27	250.38	8.46

V. NUMERICAL RESULTS

The critical buckling load values of (10,10) carbon nanotube-reinforced composite beams with four commonly used end supports are presented in this section corresponding to different types of beam theories and carbon nanotube volume fractions. Polyethylene was used as the matrix material with $E^m = 3.22\ GPa$, $\nu_m = 0.3$ at the room

temperature. For the (10,10) armchair SWCNT as the reinforcement, it was assumed that $E_{11}^{CNT} = 600\,GPa$, $E_{22}^{CNT} = 10\,GPa$, $G_{12}^{CNT} = 5\,GPa$, $\nu_{CNT} = 0.19$ [19], [20].

Through matching the elastic moduli calculated by the mixture rule and those obtained directly from MD simulations, the carbon nanotube efficiency parameters were extracted which are given in Table II relevant to both short and long SWCNT reinforcements with various values of carbon nanotube volume fractions. It is worth mentioning that for the case of shear modulus, it was assumed that $\vartheta_3 = \vartheta_2$. by comparing the values of longitudinal and transverse Young's moduli predicted by the mixture rule and MD simulation, it was observed that with proper selection of ϑ_1 andϑ_2, the mixture rule had an excellent capability to predict the elastic properties of nanocomposites.

TABLE II
PROPER VALUES OF CARBON NANOTUBE EFFICIENCY PARAMETERS

Carbon nanotube volume fraction	ϑ_1	ϑ_2
Short-carbon nanotube reinforcement		
5%	0.0254	1.0351
10%	0.0443	1.2854
15%	0.0628	1.7798
25%	0.0740	1.8751
Long-carbon nanotube reinforcement		
5%	2.1577	1.1767
10%	1.6354	1.4765
15%	1.6868	2.0588
25%	1.6531	2.1820

TABLE III
CRITICAL BUCKLING LOAD OF NANOCOMPOSITE BEAM REINFORCED BY SHORT-SWCNT WITH SIMPLY SUPPORTED-SIMPLY SUPPORTED BOUNDARY CONDITIONS ($10^6\ N$)

Aspect ratio (L/h)	Carbon nanotube volume fraction	Euler-Bernoulli beam theory	Timoshenko beam theory	Reddy beam theory
	0%	0.2910	0.2830	0.2830
	5%	0.3440	0.3337	0.3337
10	10%	0.4990	0.4822	0.4822
	15%	0.7504	0.7241	0.7241
	25%	1.2003	1.1427	1.1428
	0%	0.0728	0.0719	0.0722
	5%	0.0860	0.0853	0.0853
20	10%	0.1247	0.1237	0.1237
	15%	0.1876	0.1859	0.1859
	25%	0.3001	0.2963	0.2963
	0%	0.0116	0.0116	0.0116
	5%	0.0138	0.0137	0.0137
50	10%	0.0200	0.0199	0.0199
	15%	0.0300	0.0300	0.0300
	25%	0.0480	0.0479	0.0479

The values of critical axial buckling load of composite beams reinforced by short-(10,10) SWCNT with thickness of $h = 0.1\,m$ and various aspect ratios and carbon nanotube volume fractions are presented in Table III corresponding to simply supported-simply supported boundary conditions.

The same results for composite beams reinforced by long-(10,10) SWCNT are presented in Table IV. It can be found from the results that the stiffness of nanoconposite beam reinforced with long-SWCNT was higher than the counterparts reinforced with short-SWCNT.

TABLE IV
CRITICAL BUCKLING LOAD OF NANOCOMPOSITE BEAM REINFORCED BY LONG-SWCNT WITH SIMPLY SUPPORTED-SIMPLY SUPPORTED BOUNDARY CONDITIONS ($10^6\ N$)

Aspect ratio (L/h)	Carbon nanotube volume fraction	Euler-Bernoulli beam theory	Timoshenko beam theory	Reddy beam theory
	0%	0.2911	0.2830	0.2830
	5%	6.1053	4.1142	4.1224
10	10%	9.0660	5.8485	5.8621
	15%	13.8224	8.7641	8.7859
	25%	22.2455	12.3440	12.3967
	0%	0.0734	0.0719	0.0723
	5%	1.5258	1.3613	1.3618
20	10%	2.2661	1.9924	1.9933
	15%	3.4559	3.0203	3.0211
	25%	5.5610	4.6316	4.6342
	0%	0.0117	0.0124	0.0124
	5%	0.2441	0.2401	0.2401
50	10%	0.3638	0.3546	0.3546
	15%	0.5532	0.5405	0.5405
	25%	0.8904	0.8620	0.8620

Also it was observed that by incorporating the influence of transverse shear strains in Timoshenko and Reddy beam theories, the values of critical buckling load would be reduced from those of Euler-Bernoulli beam theory relevant to all carbon nanotube volume fraction specifically for the beams with lower aspect ratios. Furthermore, the difference between critical buckling loads predicted Timoshenko and Reddy beam theories was relatively more significant corresponding to lower aspect ratios.

It can be observed from the results that an increase in the carbon nanotube volume fraction resulted in higher critical buckling load for both short- and long-SWCNT reinforced composite beams, but it was more significant for the latter.

VI. CONCLUDING REMARKS

In this work, buckling behavior of carbon nanotube-reinforced composite beams was studied under four common sets of boundary conditions including simply supported-simply supported, clamped-clamped, clamped-simply supported, and clamped-free. Both short- and long-SWCNT reinforcements were considered in the study based on different types of beam theory. The mixture rule in along with generalized differential quadrature method to discretize the constitutive differential equations was employed to obtain critical buckling loads of the nanocomposite beams. To assign proper values for carbon nanotube efficiency parameters used in the mixture rule, the elastic moduli relevant to both composites with short- and long-SWCNT reinforcements were evaluated using molecular dynamics simulation, the results of which were fitted with those obtained from the rule of mixture.

It was shown that there were various carbon nanotube efficiency parameters corresponding to different values of carbon nanotube volume fraction. It was also observed that for

higher values of carbon nanotube volume fraction, the stiffness of nanocomposite beam increased more in the case of long-SWCNT reinforcement compared to the short-SWCNT one.

REFERENCES

[1] S. Iijima, 1991, Helical Microtubes of Graphite Carbon, Nature 354, pp. 56-58.
[2] K. Liao and S. Li, 2001, Interfacial Characteristics of a Carbon Nanotube-Polystyrene Composite System, Applied Physics Letters 79, pp. 4225-4227.
[3] C. Wei, K. Cho, and D. Srivastava, 2001, Chemical Bonding of Polymer on Carbon Nanotube, MRS 2001 Meeting proceeding.
[4] K. Lau, 2003, Interfacial Bonding Characteristics of Nanotube/Polymer Composites, Chemical Physics Letters 370, pp. 399-405.
[5] E. Hammel, X. Tang, M. Trampert, T. Schmitt, K. Mauthner, and A. Eder, 2004, Carbon Nanofibers for Composite Applications, Carbon 42, pp. 1153-1158.
[6] Y. Han and J. Elliott, 2007, Molecular Dynamics Simulations of the Elastic Properties of Polymer/Carbon Nanotube Composites, Computational Materials Science 39, pp. 315-323.
[7] A. Labuschange, N.F.J. Van Rensburg, and A.J. Van der Merwe, 2009, Comparison of Linear Beam Theories, Mathematical and Computer Modelling 49, pp. 20-30.
[8] H.S. Shen, 2009, Nonlinear Bending of Functionally Graded Carbon Nanotube-Reinforced Composite Plates in Thermal Environments, Composite Structures 91, pp. 9-19.
[9] H. Haftchenari, M. Darvizeh, A. Darvizeh, R. Ansari, and C.B. Sharma, 2007, Dynamic Analysis of Composite Cylindrical Shells using Differential Quadrature Method (DQM), Composite Structures 78(2), pp. 292-298.
[10] P. Malekzadeh and A.R. Fiouz, 2007, Large Deformation Analysis of Orthotropic Skew Plates with Nonlinear Rotationally Restrained Edges using DQM, Composite Structures 80(2), pp. 196-206.
[11] M.A. De Rosa, N.M. Auciello, and M. Lippiello, 2008, Dynamic Stability Analysis and DQM for Beams with Variable Cross-Section, Mechanics Research Communications 35(3), pp. 187-192.
[12] Y.J. Hu, Y.Y. Zhu, and C.J. Cheng, 2009, DQM for Dynamic Response of Fluid-Saturated Visco-Elastic Porous Media, International Journal of Solids and Structures 46(7-8), pp. 1667-1675.
[13] O. Sepahi, M.R. Forouzan, and P. Malekzadeh, 2010, Large Deflection Analysis of Thermo-Mechanical Loaded Annular FGM Plates on Nonlinear Elastic Foundation via DQM, Composite Structures 92(10), pp. 2369-2378.
[14] S.C. Pradhan and T. Murmu, 2010, Application of Nonlocal Elasticity and DQM in the Flapwise Bending Vibration of a Rotating Nanocantilever, Physica E 42(7), pp. 1944-1949.
[15] I. Hanasaki, A. Nakatani, and H. Kitagawa, 2004, Molecular Dynamics Study of Ar Flow and He Flow Inside Carbon Nanotube Junction as a Molecular Nozzle and Diffuser, Science and Technology of Advanced Materials 5, pp. 107-113.
[16] K. Bi, Y. Chen, J. Yang, Y. Wang, and M. Chen, 2006, Molecular Dynamics Simulation of Thermal Conductivity of Single-Wall Carbon Nanotubes, Physics Letters A 350, pp. 150-153.
[17] Nanorex Inc., 2005, NanoHive-1 v.1.2.0-b1, www.nanoengineer-1.com
[18] S.J. Stuart, A.B. Tutein, and J.A. Harrison, 2000, A Reactive Potential for Hydrocarbons with Intermolecular Interactions, Journal of Chemical Physics 112, pp. 6472-6486
[19] C.F. Cornwell and L.T. Wille, 1997, Elastic Properties of Single-Walled Carbon Nanotubes in Comparison, Solid State Communications 101, pp. 555-558.
[20] V.N. Popov, V.E. Van Doren, and M. Balkanski, 2000, Elastic Properties of Crystals of Single-Walled Carbon Nanotube, Solid State Communications 114, pp. 395-399.